Kinetics of Precipitation of Calcium Carbonate in Alkaline pH at Constant Supersaturation. Spontaneous and Seeded Growth

Nikos Spanos and Petros G. Koutsoukos*

Institute of Chemical Engineering and High-Temperature Chemical Processes, Department of Chemical Engineering, University of Patras, GR 265 00 Patras, Greece

Received: February 17, 1998; In Final Form: April 14, 1998

The seeded and unseeded precipitation of calcium carbonate from supersaturated aqueous solutions was investigated in a closed system under conditions of constant supersaturation (supersaturation 1.88−3.39) at 25 °C and at pH 9.0 and 10.0. The analysis of our results based on expressions for the supersaturation dependence of the induction time in seeded and unseeded precipitation according to the classical nucleation theory provides additional information on the mechanism of crystal growth and nucleation of calcium carbonate from supersaturated solutions. High pH values and relatively high supersaturations favor the precipitation of vaterite. The induction times were shorter in the seeded precipitation compared to those in the unseeded precipitation and displayed a marked inverse dependence on the solution supersaturation. Crystal growth proceeds via the spiral growth mechanism. The relatively low surface energy calculated for vaterite from the kinetics data, and the very low nucleation rate constant, indicate that some degree of heterogeneous nucleation occurs. A model equation describing the kinetics of precipitation of vaterite was derived by using the rate constants for nucleation and growth. According to this equation, crystal growth and nucleation predominate at relatively low and high supersaturations, respectively. In all cases examined the process was controlled by the diffusion of the growth units of calcium carbonate on the surface of the supercritical nuclei and/or the crystals inoculating the supersaturated solutions. Finally, it was found that kinetics of precipitation is independent of pH over the range investigated. The effect of pH is restricted to the supersaturation ratio which increases with pH.

Introduction

The precipitation of calcium carbonate in aqueous supersaturated solutions is of great interest both from the fundamental and from the applications point of view. To a large extent the particular interest in this system is due to the polymorphism of calcium carbonate, which besides the hydrated salts may be found as vaterite, aragonite, and calcite in order of decreasing solubility and increasing stability. The three polymorphs have markedly different physicochemical characteristics, and it is often found that less stable forms are stabilized kinetically[1−3] and/or biochemically (aragonite shells). Investigations of the transformation of the less stable polymorphs to the thermodynamically most stable calcite are often faced with the problem of rapidly changing supersaturation during the course of calcium carbonate precipitation.[4−8] Supersaturation is a key factor contributing to the stabilization of the polymorphic phases of calcium carbonate. It has been proposed that the relative abundance of the polymorphs may be explained by changes of the activity product in the aqueous phase and the transformation of the less stable polymorphic phases.

In the present work we have overcome the problems caused by the variation of the solution supersaturation during the formation of calcium carbonate by carrying out the experiments at constant supersaturation.[1,9,10] The experiments were done at a pseudo-steady state in which the driving force was kept constant by the addition of titrant solutions with the stoichiometry of the precipitating salt. It was thus possible to measure sensitive kinetic parameters such as the induction times preceding the onset of precipitation and the rates of crystal growth of calcium carbonate with the maximum possible accuracy and reproducibility. A kinetic model was obtained through the determination of the kinetic parameters, in the manner suggested by Kaschiev and co-workers.[11−13] The present work reports on the results obtained in supersaturated solutions at pH 9.0 and 10.0 for stoichiometric concentrations of total calcium and total carbonate according to the precipitating solid and at conditions of constant supersaturation.

Experimental Section

The experiments were done in double-walled, water-jacketed, thermostated Pyrex vessels, volume totaling $V = 0.22$ dm^3 at 25.0 ± 0.1 °C. The system was closed to the atmosphere, not allowing for exchange of CO_2. Stock calcium nitrate and sodium nitrate solutions were prepared from the respective solids (Merck, Puriss.) using triply distilled water. Sodium bicarbonate stock solutions were prepared fresh for each experiment from the solid reagent (Riedel de Haen AG). Equal volumes (0.1 dm^3) of calcium nitrate and sodium bicarbonate prepared from the respective stock solutions were simultaneously added (mixing time ca. 15 s) into the reaction vessel under magnetic stirring at 250 rpm. Variation of the stirring up to 400 rpm did not cause any significant difference in our measurements. Immediately following mixing, the pH of the supersaturated solutions was adjusted through the addition of standard potassium hydroxide solution. The pH measurement, calibration of the glass/saturated calomel electrode pair used, and stock solution standardization have been described in detail elsewhere.[1,2] Following pH adjustment, the solutions were stable

S1089-5647(98)01171-7 CCC: $15.00
Published on Web 07/29/1998

for an adequately long time period, as verified by the constancy of the solution pH. Moreover, the constancy of the solution pH provided for an additional verification of the validity of our assumption that the system was closed to the atmosphere, not allowing for exchange in CO_2. After the lapse of easily measurable and reproducible (better than 10%, mean of four experiments) induction times, precipitation accompanied by proton release in the bulk solution started. A decrease in the solution pH as small as 0.003 pH units triggered the addition of titrant calcium nitrate and sodium carbonate solutions having the stoichiometry (1:1) of the precipitating $CaCO_3$. The additions were done from the two mechanically coupled precision glass, calibrated burets of a computer-controlled automatic titration system. In the titrant solutions the appropriate reagents were added to avoid dilution of the working supersaturated solutions and changes in the ionic strength. The composition of the titrant solutions, calculated so as to maintain the solution supersaturation throughout the course of the precipitation experiments, has been described in detail elsewhere.[3]

During the course of the precipitation process, samples of ca. 8 mL were withdrawn at random, so as to keep approximately a constant volume, and were filtered through membrane filters (Millipore 0.2 μm). The filtrates were analyzed for calcium by atomic absorption spectrometry (Perkin-Elmer 305 A) in order to confirm the constancy of the solution composition. In all experiments the analysis showed that during crystallization the calcium concentration remained constant to within $\pm$3%. The solid precipitates were characterized by powder X-ray diffraction (XRD Philips 1830/40) and scanning electron microscopy (SEM, JEOL JSM 5200). The particle number and size distribution of the precipitate were measured by a counter based on laser radiation scattering (Spectrex ILI 1000).

A series of vaterite crystal growth experiments were conducted by seeding supersaturated solutions described above. In these experiments, stable supersaturated solutions were prepared as mentioned above. Following the verification of the stability of the solutions by monitoring a constant value of pH for at least 2 h, the crystallization was induced by the addition of vaterite seed crystals.

The seeds of vaterite used in the seeded precipitation experiments were prepared from unseeded precipitation experiments at pH = 10.0 by using the method of continuous crystallization at constant supersaturation and were characterized by powder X-ray diffraction and scanning electron microscopy following their drying at room temperature. The added seed mass was ca. 5 mg and was weighed accurately before its addition ($\pm$0.1 mg).

The rates of precipitation were measured directly from the volume of titrants added as a function of time (mol/min). Since the solution supersaturation was kept constant, the recording of titrants added as a function of time for each supersaturation corresponded to the amount of calcium carbonate formed with time. For the seeded growth experiments the rates were normalized per unit surface area of the seed crystals (specific surface area 1 $m^2\ g^{-1}$) while for the unseeded the normalization was done according to the amount precipitated, assuming that the specific surface area of the nucleating phase was constant throughout and approximately equal to 1 $m^2\ g^{-1}$, value measured for the precipitate collected at the end of the experiments.

Results

The driving force for the formation of a calcium carbonate polymorph, *x*, is defined as the change in Gibbs free energy for going from the supersaturated solution to equilibrium:

$$\Delta G_x = -R_g T \ln S_x \tag{1}$$

where R_g is the gas constant, T is the absolute temperature, and S_x is the supersaturation ratio:

$$S_x = \{(Ca^{2+})(CO_3^{2-})/K^0_{S,x}\}^{1/2} \tag{2}$$

In eq 2, parentheses denote activities and $K^0_{S,x}$ is the thermodynamic solubility product of the polymorph *x*. It is obvious that calculation of the supersaturation ratio requires computation of the solution speciation by taking into account all equilibria, mass balance, and the electroneutrality condition. All calculations of the speciation and driving forces in the present work were done using the computer program HYDRAQL.[14] In all cases, the complicating gas/ liquid equilibrium of carbon dioxide was neglected by choosing relatively large solution volumes, high pH, and minimal air volume above the aqueous phase.[15] The physicochemical examination by powder XRD and SEM of the solid precipitates showed that the thermodynamically unstable vaterite formed in both seeded and unseeded experiments. The formation of vaterite under similar conditions, i.e., pH 9.0 and 10.0 at temperature 25 °C, has been already reported in the literature.[11,16,17]

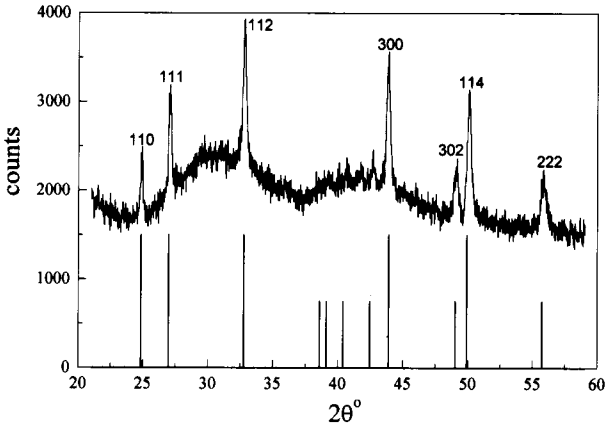

Figure 1. Typical powder XRD spectrum of the solid precipitates of this study. Characteristic reflections of vaterite are shown by vertical lines [ref 18].

In Figure 1 the XRD spectrum typical of the solid precipitates obtained is shown. The reflections characteristic for vaterite are also shown, and they matched those of reference materials.[18]

The morphology of the precipitates shown in the scanning electron micrographs in Figure 2 revealed the characteristic[19] spherical shape of the vaterite crystallites, suggesting a three-dimensional crystal growth for the vaterite crystallites. The kinetics analyses were therefore done with respect to vaterite.

The kinetics of precipitation was described from the curves of the titrant solutions added as a function of time. These curves were normalized per unit surface area of the solid phase forming. Typical plots describing the formation of vaterite in unseeded experiments are shown in Figure 3. In these plots, the progress of the precipitation process may be described by two linear segments. The initial part of the volume−time curves (smaller slope) corresponded to both nucleation and growth of the supercritical nuclei. The time corresponding to the intersection point of the two straight lines was defined as the induction time; that is the time needed for the formation of supercritical nuclei. In the seeded growth experiments the induction times were the time lapsed between the inoculation of the supersaturated solutions with vaterite crystals and the onset of addition of titrant

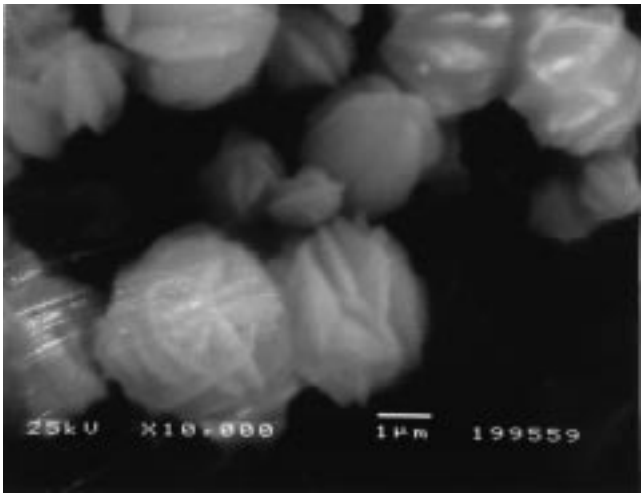

Figure 2. Typical scanning electron micrograph of the precipitating solids at conditions of constant supersaturation.

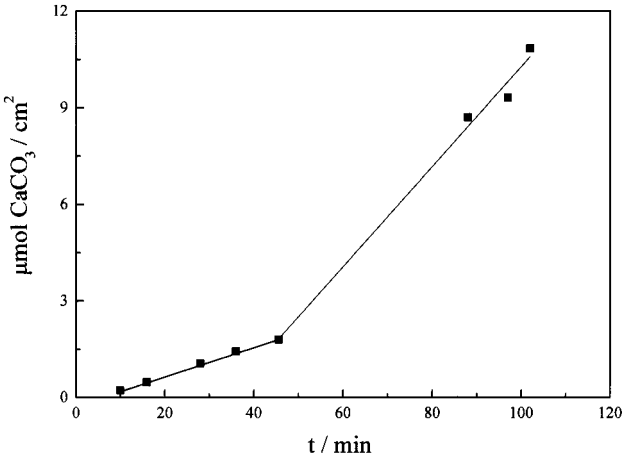

Figure 3. Variation of the amount of vaterite formed per unit area with time. Unseeded precipitation, total calcium concentration, Ca_t = total carbonate concentration, $C_t = 2 \times 10^{-3}$ M, pH = 9.0, 25.0 °C.

solutions. It should also be noted that, in seeded growth, throughout the process crystal growth occurred without secondary nucleation. This was verified by the fact that the rates measured in seeded precipitation experiments showed a linear dependence on the amount of the inoculating seeds in the supersaturated solutions, as may be seen from the results presented in Figure 4. The initial rates of precipitation, R (mol s^{-1} m^{-2}), were expressed as linear rates $\dot{r}$ (m s^{-1}):

$$\dot{r} = \mathrm{d}r/\mathrm{d}t = RM_w d^{-1} \tag{3}$$

where r is the mean radius of a sphere equivalent to the particles, M_w the molar mass of vaterite (kg mol^{-1}), and d its density (2653 kg m^{-3}).[20]

The experimental conditions, pH, total concentration of calcium, the supersaturation ratio, the measured values of the induction time, initial rates of precipitation, and their respective linear rates for the unseeded and seeded precipitation experiments are compiled in Table 1. As may be seen, the induction times decreased with increasing supersaturation while the rates of precipitation increased in both unseeded and seeded precipitation. Moreover, it may be observed that the induction times are sufficiently shorter in the seeded precipitation experiments where the precipitation rates are higher especially at high supersaturations.

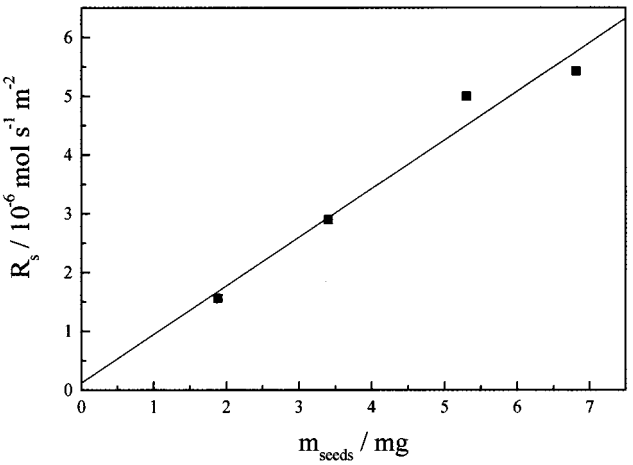

Figure 4. Initial rate of precipitation as a function of the mass of the added seeds. $Ca_t = C_t = 7 \times 10^{-4}$ M, pH = 10.0, 25.0 °C.

Discussion

According to the classical nucleation theory, both nucleation and crystal growth rates depend on the solution supersaturation. The rate constants for nucleation and crystal growth are K_J and K_G, respectively, and they do not depend on supersaturation. These constants may be calculated according to the analysis of the kinetics data presented by Verdoes et al.[11,12]

The sufficiently shorter induction time for seeded precipitation, t_s, compared with that for unseeded precipitation, t_u (Table 1), demonstrates that t_s was controlled only by the growth of the added seeds, implying that the effect of extra primary nucleation on t_s was negligible.[11] This result is in agreement with our previous conclusion that crystal growth of the added seeds predominated in the seeded precipitation. Next, we tried on this basis to specify the growth model from the seeded precipitation results, testing different expressions relating t_s with S, which corresponded to different growth models (normal growth, spiral growth, 2D nucleation-mediated growth, diffusion-controlled growth).[12] The relationship corresponding to the spiral growth mechanism described our results best in the seeded experiments:

$$t_s = A_s/(S-1)^p \tag{4}$$

A_s is a S-independent factor which in the case of large total volume of the added seeds is given by[12]

$$A_s = \alpha/mC_m r_s^{m-1} N K_G \tag{5}$$

where $m = 3$ for three-dimensional (3D) growth, C_m is a shape factor which in 3D growth of spheres equals to $4\pi/3$, r_s is the radius of the seeds estimated by SEM to be 1×10^{-6} m, N is the number density of the seeds (m^{-3}), K_G is the S-independent growth rate constant, and α is the smallest experimentally detectable volume fraction of the newly formed phase.[12] In our case α was estimated to be 5×10^{-8}.

It is obvious that A_s can be determined from eq 4 by plotting $\ln t_s$ vs $\ln(S-1)$ (Figure 5). It may be observed that the straight lines corresponding to the best fit lines obtained from linear regression of $\ln t_s$ vs $\ln(S-1)$ describe very well our results obtained in seeded experiments for both pH values. The slopes, intercepts, values of A_s calculated from the intercept, and values of K_G calculated from A_s (eq 5) are summarized in Table 2. The slopes of the best fit lines, given in Table 2, indicate a spiral growth mechanism (parabolic law)[21,22] at both pH values

TABLE 1: Total Concentration of Calcium (Equal to Total Carbonate), Supersaturation Ratio, *S*, Induction Time, *t*, and Initial Rate of Precipitation, Obtained at Two pH Values for the Unseeded (Subscript u) and Seeded (Subscript s) Precipitation

pH	$C_{ca,t}/10^{-3}$ M	S	t_u/ min	t_S/ min	$R_u/10^{-5}$ mol s^{-1} m^{-2}	$R_S/10^{-5}$ mol s^{-1} m^{-2}	$(dr/dt)_u$/nm s^{-1}	$(dr/dt)_s$/nm s^{-1}
9.0	1.5	1.88	140	34	0.2	0.4	0.08	0.16
9.0	1.6	2.02	108	28	0.4	0.8	0.14	0.29
9.0	1.8	2.17	90	22	0.5	0.9	0.20	0.33
9.0	2.0	2.36	45	16	0.7	1.3	0.28	0.50
9.0	2.5	2.81	15	10	1.2	4.2	0.44	1.57
9.0	3.0	3.22	5		4.5		1.70	
10.0	0.4	1.51	108	76	0.2	0.2	0.08	0.09
10.0	0.6	1.89	57	43	0.3	0.3	0.13	0.13
10.0	0.7	2.12	34	24	0.4	0.5	0.17	0.17
10.0	0.8	2.34	19	12	0.5	0.8	0.19	0.31
10.0	1.0	2.75	12	7	1.3	6.5	0.50	2.46
10.0	1.3	3.39	7		4.7		1.76	

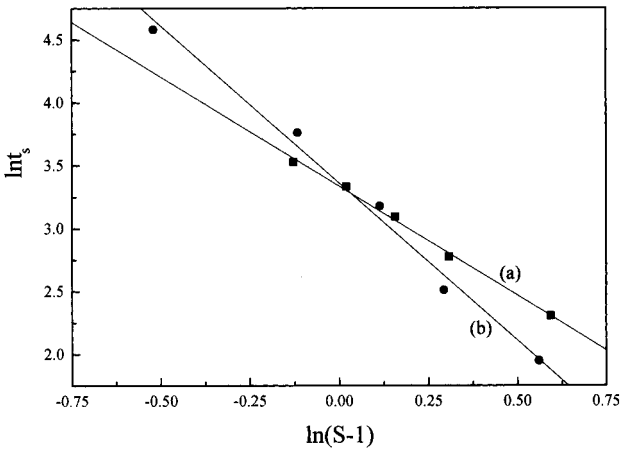

Figure 5. Plot of the logarithm of the induction time as a function of the logarithm of the supersaturation with respect to vaterite. pH = 9.0 (curve a) and pH = 10.0 (curve b), 25.0 °C.

TABLE 2: Results of Regression Analysis of ln t_s vs ln(S − 1) as Well as Calculated Values of A_s and K_G for the Seeded Precipitation at Two pH Values

pH	slope	intercept	A_S/ min	K_G/ m s^{-1}
9.0	1.74	3.33	27.9	1.06×10^{-10}
10.0	1.98	3.21	24.6	1.17×10^{-10}

9.0 and 10.0. The same mechanism for vaterite has also been reported in the literature at conditions of variable supersaturation.[17,19,23]

The K_G values obtained in our work (1.06×10^{-10} and 1.17×10^{-10} m s^{-1}) are comparable with the experimental value $K_G = 5.6 \times 10^{-10}$ m s^{-1} reported in the literature,[19] which in turn is comparable to the value $K_G = 1.9 \times 10^{-10}$ m s^{-1} calculated theoretically.[24]

Regarding the growth model in the unseeded precipitation, expressions between t_u and S corresponding to different models were tested. It was found that the relationship corresponding to spiral growth (linear law)[11,12] described very well our experimental results at both pH values:

$$t_u = A_u(S-1)^{-3/4}S^{-1/4}\exp(B/4\ln^2 S) \quad (6)$$

In the above equation

$$B = C_m\sigma^3 v^2(kT)^3 \quad (7)$$

where v is the molecular volume and σ is the interfacial tension. A_u is an S-independent factor given by

$$A_u = (3\alpha/\pi K_J K_G^3)^{1/4} \quad (8)$$

where K_J is the S-independent nucleation constant.

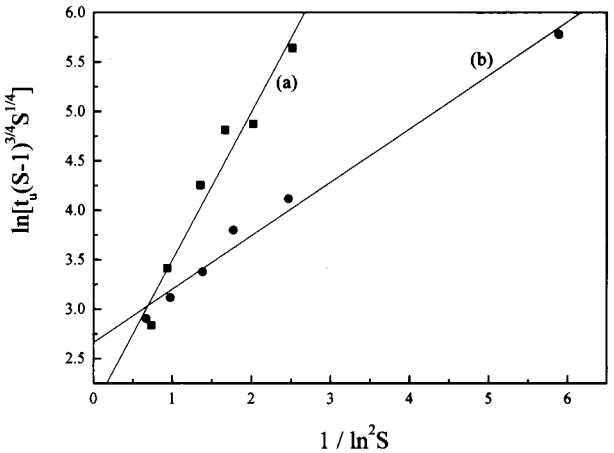

Figure 6. Plot of $\ln[t_u(S-1)^{3/4}S^{1/4}]$ as a function of $1/\ln^2 S$. pH = 9.0 (curve a) and pH = 10.0 (curve b), 25.0 °C.

TABLE 3: Results of Regression Analysis of $\ln[t_u(S-1)^{3/4}S^{1/4}]$ vs $1/\ln^2 S$ and the Calculated Parameters K_J, σ, and n^* for the Unseeded Precipitation at Two pH Values

pH	intercept	slope	A_u/min	K_J/ m^{-3} s^{-1}	σ/mJ m^{-2}	n^*
9.0	2.07	1.35	7.9	2.2×10^{11}	45.1	3.4−21.4
10.0	3.07	0.24	21.5	2.8×10^{9}	25.4	0.5−13.7

By plotting $\ln[t_u(S-1)^{3/4}S^{1/4}]$ vs $1/\ln^2 S$ (Figure 6), we observe that eq 6 describes our results very well at both pH values. The results of the regression analysis according to eq 6 are given in Table 3. From the intercept, ln A_u, we may calculate the nucleation rate constant, K_J, by using eq 8 and the growth rate constant, K_G, determined from the seeded precipitation analysis (Table 2). The thermodynamic constant B may be calculated from the respective slopes, $B/4$. From the value of B, the interfacial tension σ for the phase forming may be calculated from eq 7 as well as the number of molecules or formula units in the 3D critical nucleus, n^*, using the relation[25]

$$n^* = B/\ln^3 S \quad (9)$$

The values of the parameters calculated as described above are summarized in Table 3.

The theoretical interfacial tension computed for homogeneous vaterite nucleation[19,24] is $\sigma = 90$ mJ m^{-2}. Verdoes et al.,[11] Kralj et al.,[19] and Gomez et al.[17] reported σ values for vaterite formation equal to 37.3, 34, and 40.7 mJ m^{-2}, respectively. They ascribed the relatively low value of σ to some degree of heterogeneous nucleation. According to Söhnel and Mullin[26] and Nielsen and Söhnel,[27] very low σ values correspond to heterogeneous nucleation while very high σ values correspond to erroneous assumptions in the data treatment. Our σ values (Table 3) are comparable with the values obtained by Verdoes

et al., Kralj et al., and Gomez et al. for vaterite and in comparison with the theoretical value of 90 mJ m^{-2} indicate that some degree of heterogeneous nucleation cannot be precluded. Moreover, the calculated relatively low number of molecules participating in the formation of the 3D critical nucleus, n^* (Table 3), is comparable with the relatively low n^* values reported in the literature.[11,17] Finally, the K_J values obtained at both pH values (Table 3) are lower than those obtained by Verdoes et al.[11] and Gomez et al.,[17] which were $K_J = 1.4 \times 10^{18}$ and 2.9×10^{20} m^{-3} s^{-1}, respectively. They are also much lower than the theoretical expected $K_J \approx 10^{31}-10^{36}$ m^{-3} s^{-1} for homogeneous nucleation in solution.[25,28] This is an additional indication of some degree of heterogeneous nucleation in the system studied.

From the nucleation and crystal growth constants K_J and K_G a model equation describing the kinetics of precipitation was obtained. In the calculation of the initial rates of spontaneous precipitation it was considered that both nucleation and crystal growth take place.[29] The expression for 3D nucleation rates according to the classical nucleation theory (e.g., ref 25)

$$J = K_J S \exp(-B/\ln^2 S) \tag{10}$$

may be transformed into a linear rate as follows:

$$J = K_J V r^* S \exp(-B/\ln^2 S) \tag{11}$$

where r^* is the radius of the critical nucleus (m) defined as[25]

$$r^* = \sigma v/(kT \ln S) \tag{12}$$

Combination of eqs 11 and 12 results in the nucleation rate expressed in m s^{-1}:

$$J = K_J V \sigma v \frac{S}{kT \ln S} \exp\left(-\frac{B}{\ln^2 S}\right) \tag{13}$$

In our experiments, the supersaturation was kept constant through the precipitation process, thus establishing a steady-state condition by the addition of the appropriate titrant solutions. In such conditions, both crystal growth and nucleation contribute.[30,31] The initial rates of spontaneous precipitation measured in our experiments equal the sum of the nucleation rate (eq 13) and the growth rate. As already mentioned, the growth of the crystals follows a spiral growth mechanism (parabolic law), so the growth rate, G, is given by[21,22]

$$G = K_G(S-1)^2 \tag{14}$$

Consequently, the final model equation for the linear initial rate of spontaneous precipitation is

$$\dot{r} = \frac{K_J V \sigma v}{kT} \frac{S}{\ln S} \exp\left(-\frac{B}{\ln^2 S}\right) + K_G(S-1)^2 \tag{15}$$

The testing of the derived model equation was done by comparing the initial rates of spontaneous precipitation calculated from eq 15 with the experimental values shown in the eighth column of Table 1. Figure 7 illustrates the experimental values obtained at pH 9.0 and 10.0 and the calculated values (curve a) calculated from eq 15 by using for K_J and K_G the geometrical averages of the values determined at the two pH values, i.e., 2.5×10^{10} m^{-3} s^{-1} and 1.1×10^{-10} m s^{-1}. It may be seen that eq 15 describes very well our experimental results irrespective of the pH at which they have been obtained. It should be noted that a σ value equal to 72.5 mJ m^{-2} was used,

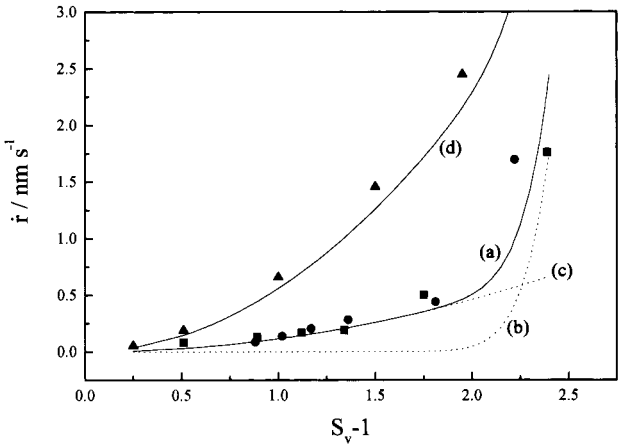

Figure 7. Experimental rates of precipitation of vaterite obtained (i) in this study at pH values 9.0 (●) and 10.0 (■) and (ii) by Kralj et al. (ref 19) (▲), as well as their fittings according to eq 15 (curves a and d). Curves c and b represent the growth and nucleation contribution to the total rate of precipitation (curve a).

which was calculated from[27]

$$\sigma = 846\left(\frac{\log S_{cr}}{V_m}\right)^{2/3} \quad \text{mJ m}^{-2} \tag{16}$$

where V_m is the molar volume (18.8 cm^3) and S_{cr} is the critical supersaturation ratio, corresponding to $J = 1$ cm^{-3} s^{-1}. The values of σ given in Table 3 are calculated from experimental measurements of the induction time as a function of the solution supersaturation (eq 6). These values are lower than the true values of surface energy because of the fact that precipitation is heterogeneous.[32] Experimentally S_{cr} may be determined as the supersaturation at which the nucleation rate starts to increase significantly. Therefore, it is necessary to analyze the initial rate of precipitation (curve a) in the two contributions, nucleation (curve b) and growth (curve c) rate. From curve b it may be inferred that $S_{cr} = 2.96$.

The validity of our model equation is confirmed by the fact that it predicts the well-known predominance of crystal growth at relatively low supersaturations and of nucleation at relatively high supersaturations (curves c and b, respectively). The validity of our model is further supported by the satisfactory fit (Figure 7, curve d) of the data of experimental rates of precipitation obtained by Kralj et al.[19] For K_G the value obtained experimentally by these authors, 5.6×10^{-10} m s^{-1}, was used.

Finally, the aforementioned finding that the growth rate is not diffusion but surface controlled may be further supported from the following considerations: According to Nielsen and Toft,[33] for a binary symmetric electrolyte where the two ions have the same ionic diffusion coefficient, the diffusion-controlled growth rate is given by

$$\dot{r}_D = \frac{2DV_m}{r}\left[\frac{C_1 + C_2}{2} - \left(\left(\frac{C_1 - C_2}{2}\right)^2 + K_s\right)^{1/2}\right] \tag{17}$$

where D is the diffusion coefficient (10^{-9} m^2 s^{-1}), r is the particle radius (10^{-6} m), and C_1, C_2 are the concentrations of the ions Ca^{2+} and CO_3^{2-}, respectively. Figure 8 shows our experimental growth rates obtained at pH 9.0 and 10.0 and the diffusion-controlled growth rates calculated from eq 17 at pH 9.0 and 10.0. The much higher diffusion-controlled rates ($\dot{r} \ll \dot{r}_D$) strongly suggest that the growth rate is determined by surface diffusion; i.e., it is surface controlled. Moreover, it should be noted that our results show that the kinetics of $CaCO_3$

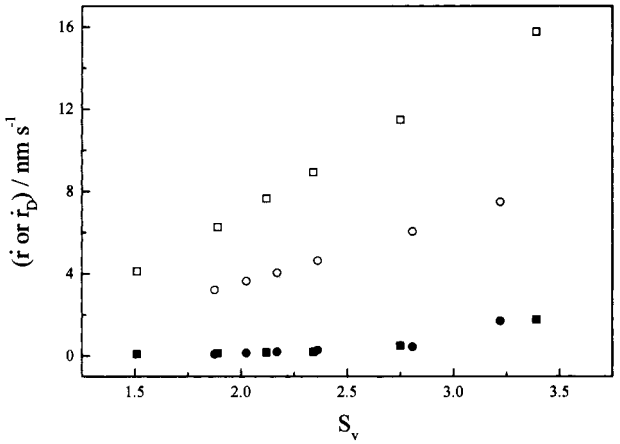

Figure 8. Experimental rates of precipitation obtained at pH values 9.0 (●) and 10.0 (■) and diffusion-controlled growth rates calculated from eq 17 at pHs 9.0 (○) and 10.0 (□).

precipitation at pH 9.0 and 10.0 do not depend on pH. Dependence of the kinetics of $CaCO_3$ crystallization has been reported al lower pH values.

Conclusions

In a series of experiments at pH 9.0 and 10.0, 25 °C, and conditions of sustained supersaturation, it was shown that $CaCO_3$ precipitates as vaterite. The technique of constant supersaturation allowed for the precise measurement of kinetic parameters, such as the induction times preceding the calcium carbonate formation in the supersaturated solutions and the subsequent rates of formation of the solid phase at sustained supersaturation. The experiments done included both spontaneous precipitation and seeded growth in which precipitation was initiated by the introduction of vaterite seed crystals. The induction times, sufficiently shorter in seeded precipitation compared with those in unseeded precipitation, are markedly inversely dependent on the solution supersaturation. The precipitation of vaterite (seeded and unseeded) is a surface-controlled process. Specifically, the analysis of induction times points at the spiral growth mechanism. The relatively low values calculated for the surface energy of vaterite suggested a certain degree of heterogeneous nucleation. The value obtained for K_J was considerably lower in comparison with the value anticipated according to the classical nucleation theory.

The determination of the rate constants for growth and nucleation, K_G and K_J, respectively, allowed for the derivation of a model equation describing the kinetics of precipitation, according to which crystal growth and nucleation predominate at relatively low and high supersaturations, respectively. The kinetics of precipitation was found to be independent of pH, for pH 9.0 and 10.0. The effect of pH was restricted to the supersaturation ratio, which increased with pH.

Acknowledgment. The authors wish to acknowledge partial financial support of this work by the General Secretarial for Research and Technology through program EPET II #514.

References and Notes

(1) Xyla, A. G.; Koutsoukos, P. G. *J. Chem. Soc., Faraday. Trans. 1* **1987**, *83*, 1477.

(2) Giannimaras, E. K.; Koutsoukos, P. G. *J. Colloid Interface Sci*. **1987**, *116*, 423.

(3) Giannimaras, E. K.; Koutsoukos, P. G. *Langmuir* **1988**, *4*, 855.

(4) Ogino, T.; Suzuki, T.; Sawada, K. *Geochim. Cosmochim. Acta* **1987**, *51*, 2757.

(5) Kralj, D.; Brecevic, L.; Nielsen, A. E. *Proc. 11th Symp. Ind. Cryst. A.* **1990**, 267.

(6) Richter, A.; Petzold, D.; Hoffmann, H.; Ulrich, B. *Chem. Tech.* **1955**, *47*, 306.

(7) Richter, A.; Petzold, D.; Ulrich, B. *Chem. Tech.* **1996,** *48*, 271.

(8) Hoffmann, H.; Wagner, S.; Ulrich, B. *Chem. Tech.* **1996**, *48*, 96.

(9) Tomson, M. B.; Nancollas, G. H. *Science* **1978,** *200*, 1059.

(10) Kazmierczak, T. F.; Tomson, M. B.; Nancollas, G. H. *J. Phys. Chem.* **1982,** *86*, 103.

(11) Verdoes, D.; Kaschiev, D.; Van Rosmalen, G. M. *J. Cryst. Growth* **1992,** *118*, 401.

(12) Van der Leeden, M. C.; Verdoes, D.; Kaschiev, D.; van Rosmalen, G. M. In *Advances in Industrial Crystallization*; Garside, J., Davey, R. J., Jones, A. G., Eds.; Butterworth-Heinemann: London, 1991; p 31.

(13) Kaschiev, D. In *Industrial Crystallization 87*; Nyvlt, J., Zacek, S., Eds.; Elsevier: Amsterdam, 1989; p 49.

(14) Papelis, C.; Hayes, K. F.; Leckie, J. O. HYDRAQL. A Program for The Computation of Chemical Equilibrium Composition of Aqueous Batch Systems Including Surface Complexation Modelling of Ion Association at the Oxide Solution Interface. Technical Report No. 306, Stanford University, Stanford, CA, 1988.

(15) Söhnel, O.; Mullin, J. W. *J. Colloid Interface Sci*. **1988**, *123*, 43.

(16) Xyla, A. G.; Giannimaras, E. K.; Koutsoukos, P. G. *Colloids Surf.* **1991,** *53*, 241.

(17) Gomez, J.; Torrent, J.; Rodriguez, R. *J. Cryst. Growth* **1996,** *169*, 331.

(18) JCPDS, File No. 13-0192.

(19) Kralj, D.; Brecevic, L.; Nielsen, A. E. *J. Cryst. Growth* **1990,** *104*, 793.

(20) *CRC Handbook of Physics and Chemistry*, 74th ed.; CRC Press: Boca Eaton, FL, 1976; p B-221.

(21) Burton, W. K.; Cabrera, N.; Frank, F. C. *Philos. Trans. R. Soc. London* **1951,** *A243*, 299.

(22) Nielsen, A. E. *Pure Appl. Chem.* **1981,** *53*, 2025.

(23) Xyla, A. G.; Mikroyannidis, J.; Koutsoukos, P. G. *J. Colloid Interface Sci*. **1992,** *153*, 537.

(24) Nielsen, A. E. *J. Cryst. Growth* **1984,** *67*, 289.

(25) Nielsen, A. E. *Kinetics of Precipitation*; Pergamon: Oxford, 1964.

(26) Söhnel, O.; Mullin, J. W. *J. Cryst. Growth* **1982,** *60*, 239.

(27) Nielsen, A. E.; Söhnel, O. *J. Cryst. Growth* **1971**, *11*, 233.

(28) Zettlemoyer, A. C., Ed. *Nucleation*; Dekker: New York, 1969.

(29) Malollari, I. Xh.; Klepetsanis, P. G.; Koutsoukos, P. G. *J. Cryst. Growth* **1995,** *155*, 240.

(30) Nyvlt, J.; Söhnel, O.; Matuchova, M.; Broul, M. *The Kinetics of Industrial Crystallization*; Elsevier Amsterdam, 1985; p 260.

(31) Söhnel, O.; Garside, J. *Precipitation*; Butterworth-Heinemann: Oxford, 1992; p 247.

(32) Mullin, J. W. *Crystallization*, 3rd ed.; Butterworth-Heinemann: Oxford, 1991; pp 194−201.

(33) Nielsen, A. E.; Toft, J. M. *J. Cryst. Growth* **1984,** *67*, 278.